

Spontaneous Formation of Uniform Cell-Sized Microgels through Water/Water Phase Separation

Mayu Shono, Gen Honda, Miho Yanagisawa,* Kenichi Yoshikawa, and Akihisa Shioi*

In this study, a one-step method is discussed for producing uniform cell-sized microgels using glass capillaries filled with a binary polymer blend of polyethylene glycol (PEG) and gelatin. Upon decreasing temperature, phase separation of the PEG/gelatin blends and gelation of gelatin occur, and then the polymer blend forms linearly aligned, uniformly sized gelatin microgels in the glass capillary. When DNA is added to the polymer solution, gelatin microgels entrapping DNA are spontaneously formed, and the DNA prevents the coalescence of the microdroplets even at temperatures above the melting point. This novel method to form uniform cell-sized microgels may be applicable to other biopolymers. This method is expected to contribute to diverse materials science via biopolymer microgels and biophysics and synthetic biology through cellular models containing biopolymer gels.

Water/oil (w/o) droplets and liposomes are often used as a prototype of cellular models in several studies, for example, the gene expression inside w/o droplets,^[7] lipid-coated w/o droplets,^[3,8,9] and construction of cell-sized giant liposomes equipped with motor proteins.^[10] Recently, water/water (w/w) droplets generated by aqueous two-phase systems (ATPS) have been used to extract, separate, and purify biomolecules and cells,^[11–13] attracting great attention to form cellular models.^[14–17] In several aspects, the w/w droplet is superior to w/o droplets as a cellular model. Unlike the w/o droplets, the w/w droplets can produce a molecular crowding environment similar to living cells through w/w phase separation by mixing binary polymer solutions, generating

microdroplets without lipids and oil. Such droplets are regarded as a simple model for membrane-less organelles in which it creates a crowded environment that is different from the external environment without a membrane coating on the surface. The most popular binary polymer solution for generating the w/w droplets is polyethylene glycol (PEG) with gelatin or dextran (DEX).^[18–22] When DNA and a lipid suspension are mixed with a binary solution of PEG and DEX, the w/w droplet can incorporate DNA, and cover its surface with a phospholipid layer like as a cell structure.^[18,20] Recent studies using PEG/DEX systems revealed

1. Introduction

Living cell is a crowded environment composed of a rich variety of biopolymers, such as DNA and proteins within a small micrometer space. Cell structures and functions emerge in a self-organized manner through the interaction of these biopolymers. The creation of a real-world cell-like model with a minimum number of components^[1–6] will contribute as a powerful approach to reduce the complexity and reveal the underlying physical principles of self-assembly.

M. Shono, A. Shioi
Department of Chemical Engineering and Materials Science
Doshisha University
6100321 Kyoto, Japan
E-mail: ashioi@mail.doshisha.ac.jp
G. Honda, M. Yanagisawa
Komaba Institute for Science
Graduate School of Arts and Sciences
The University of Tokyo
Komaba 3-8-1, Meguro, Tokyo 153-8902, Japan
E-mail: myanagisawa@g.ecc.u-tokyo.ac.jp

M. Yanagisawa
Center for Complex Systems Biology
Universal Biology Institute
The University of Tokyo
Komaba 3-8-1, Meguro, Tokyo 153-8902, Japan
M. Yanagisawa
Graduate School of Science
The University of Tokyo
Hongo 7-3-1, Bunkyo, Tokyo 113-0033, Japan
K. Yoshikawa
Faculty of Life and Medical Sciences
Doshisha University
6100394 Kyoto, Japan
K. Yoshikawa
Center for Integrative Medicine and Physics
Institute for Advanced Study
Kyoto University
606 8501 Kyoto, Japan

 The ORCID identification number(s) for the author(s) of this article can be found under <https://doi.org/10.1002/sml.202302193>

© 2023 The Authors. Small published by Wiley-VCH GmbH. This is an open access article under the terms of the Creative Commons Attribution-NonCommercial License, which permits use, distribution and reproduction in any medium, provided the original work is properly cited and is not used for commercial purposes.

DOI: 10.1002/sml.202302193

that a long-stranded DNA is localized to DEX-rich phase, while the oligomer DNA is not. This length dependence of the DNA distribution can be explained in terms of the depletion effect^[23,24] of the polymers.^[19]

In general, the main mechanisms of w/w phase separation in a binary polymer solution are the entropic effect on the freedom of the polymer molecules in a relatively dense condition, called depletion effect,^[23,24] and the enthalpic effect due to the molecular interaction among the different polymers. The ATPS system finally results in a macroscopic phase separation with minimum interfacial energy. Therefore, w/w droplets of ATPS coalesce with the neighboring droplets and gradually grow in size. To use the w/w droplets as a cellular model, the regulation of the droplet size, structural stability, and isolation by fusion inhibition among the droplets are essential because the reaction efficiency of gene expression inside the droplet depends on the droplet size.^[7]

To this date, by using microchannels with complicated and high-cost equipment, such as Nano Electro Mechanical Systems (NEMS),^[25–30] microdroplets of PEG/gelatin ATPS system ranging from 1 to 1×10^{-3} mm have been successfully produced in a size-controlled manner,^[25] and its application to microreactors is also attempted.^[26] However, these methods are challenging, time-consuming, and expensive to produce uniform droplets. To solve these issues, we have previously reported that ATPS of confined polymer blends can be utilized for the size control of w/w droplets.^[31] The phase separation of PEG/DEX solution inside a glass capillary produces cell-sized droplets with approximately uniform size through spinodal decomposition^[32] within the confinement of quasi-1D. We used this ATPS method to produce uniform cell-sized microgels. The microgels incorporating biopolymers, such as DNA and bioactive chemical species have been actively applied to biological and medical usages for advantages, such as protecting DNA from degradation, minimizing DNA loss, preventing harmful side effects, and improving DNA targeting.^[33–37] The microgels were prepared by phase separation of PEG/gelatin blends and subsequent gelation of the gelatin-rich phase. The capillary surface should be modified to preferentially attract the PEG-rich phase to the surface, generating and stabilizing the gelatin-rich droplets. When the temperature exceeds the sol/gel transition point, the DNA-containing droplets maintain their size without melting and fusing, suggesting that the incorporation of DNA molecules stabilizes the structure of the gelatin gel.

2. Results

As shown in **Figure 1a**, toward the spontaneous formation of uniform cell-sized gelatin microgels, we encapsulated a homogeneous PEG/gelatin blend solution into a glass capillary at 65 °C, which is above the transition temperatures of liquid–liquid phase separation (LLPS) and gelation of gelatin. The glass surface was coated with PEG to preferentially attract the PEG-rich phase to the surface rather than the gelatin, which has a high affinity for glass. By decreasing the temperature to 24 °C, the gelatin-rich domain transit to the gel phase. **Figure 1b,c** shows the w/w phase separation inside the b) PEG-coated and c) non-coating glass capillaries (inner diameter: 140 μm). The solution composition used was PEG:gelatin = 3.4 weight volume⁻¹% (wt vol⁻¹%):4.5 wt vol⁻¹%, which was within a phase separation

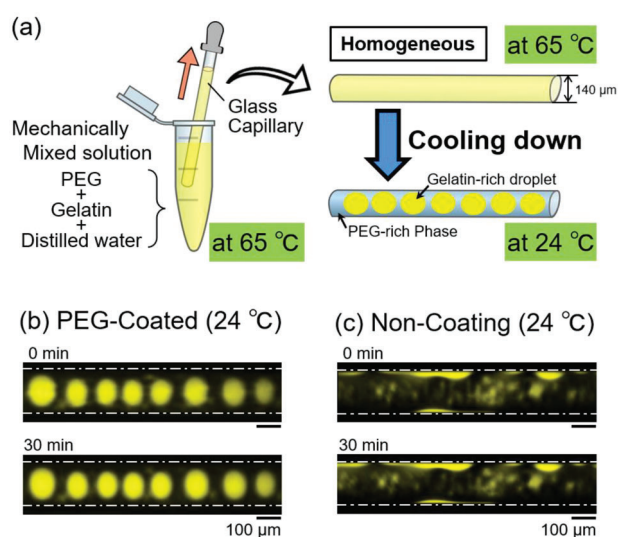


Figure 1. Experimental scheme of w/w phase separation in a capillary. a) A schematic representation of the experimental procedure. Immediately after mixing, the PEG/gelatin solution (at 65 °C) was sucked up into a PEG-coated glass capillary, and then both ends were sealed. The capillary was quenched at room temperature (≈ 24 °C). Effect of PEG-coated glass capillaries on phase separation patterns of the PEG/gelatin solutions. (Inner capillary diameter: 140 μm). The yellow region corresponds to the gelatin-rich droplets or gel phase. Dashed lines indicate the inner glass wall. b) In the PEG-coated capillary, the uniformly sized droplets of the gelatin-rich phase were linearly arranged. c) In the non-coating capillary, gelatin adhered to the glass, and the isolated droplets did not appear.

region, and the gelatin-rich domains emerged in the PEG-rich phase. **Figure 1b** shows approximately uniform cell-sized gelatin-rich droplets generated inside the PEG-coated capillary. The gelatin-rich droplets were arranged linearly along the long axis of the capillary and stable in size. In the glass capillary without the coating (**Figure 1c**), the gelatin-rich phase adhered to the glass surface and did not form uniformly sized microgels.

Figure 2a,b shows the effect of capillary confinement on the diameter of the obtained gelatin microgels. The microgels extracted from the capillary to the bulk water are also shown (**Figure 2a(i,ii)**). The fluorescent green region represents the DNA molecules. As shown in the right panel in the upper **Figure 2a**, DNA molecules were localized inside the microgels. The results showed that the gelatin-rich droplets spontaneously entrapped DNA molecules through the phase separation of PEG and gelatin. In addition, the diameter of microgels was almost the same as that of the glass capillary (inner diameter (ID): 90 and 140 μm). Therefore, smaller microgels can be produced using a capillary with a smaller inner diameter. The experimental results for the PEG-coated glass capillaries with the larger diameters (280 and 440 μm) are shown in **Figure S1** (Supporting Information), indicating that the uniformly sized microgels tend to be distributed with an increase in the inner diameter of the capillary. The lower panels in **Figure 2a** show the nearly uniform cell-sized microgels entrapping DNA extracted from the capillary. The size of the droplets did not largely change by the extraction from the glass capillary (**Figure 2a(i,ii)**). **Figure 2b** shows the microgels formed between two PEG-coated glass slides (confinement size: 3×18 mm, sandwiched between two glasses with

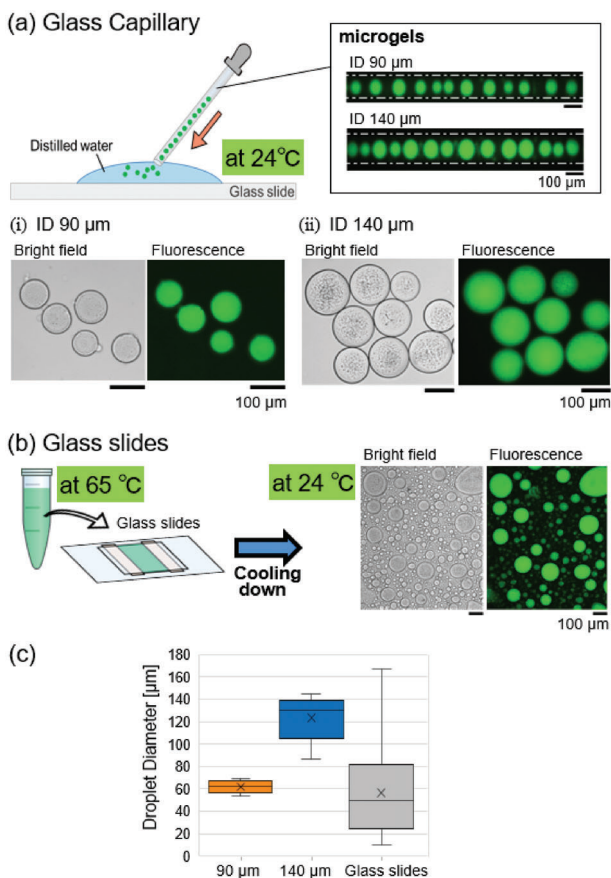


Figure 2. a) Extraction of microgels from the glass capillary. In the upper right panel: microgels entrapping DNA in a capillary (inner diameter (ID): 90 and 140 μm). i,ii) Microgels entrapping DNA pushed out into a 2 μL distilled water placed on a glass slide at room temperature (24 $^{\circ}\text{C}$) from two different capillary diameters. The green region of the fluorescent images corresponds to DNA. b) PEG/gelatin solution and DNA were mixed at 65 $^{\circ}\text{C}$ and cooled at room temperature (24 $^{\circ}\text{C}$) in the PEG-coated glass slides with an approximate depth of 90 μm . The solution composition was identical to that used in (a). c) Mean value (\bar{x}) and distribution (bar) of microgels were shown as box plots. The mean \pm standard deviation (SD) and the number of microgels (n) used in the analysis for microgel diameters were $61.7 \pm 5.3 \mu\text{m}$ ($n = 5$), $123.4 \pm 19.2 \mu\text{m}$ ($n = 9$), and $56.5 \pm 39.2 \mu\text{m}$ ($n = 49$) for the ID 90 μm capillary, 140 μm capillary, and glass slides (depth: 90 μm), respectively. The difference in mean of microgel diameters extracted from the different capillary sizes between 90 and 140 μm was $***P < 0.001$, t -test. (See the Statistical Analysis section for details).

a 0.1 mm spacer). In this setup, the size of the droplets generated was widely distributed (Figure 2b). The mean value and distribution of microgels diameter were plotted in Figure 2c. The results demonstrate that the diameter of microgels was similar to that of the inner diameter of the glass capillary, and the dispersion of diameters was much smaller for the capillary-used method. Although microgels likely expanded slightly due to osmotic pressure when extracted from the capillary, the expansion could be controlled by selecting the inner diameter of the capillary.

Figure 3 shows the fluorescence images of gelatin-rich droplets in the sol state at 33 $^{\circ}\text{C}$, which is above the gelation temperature of gelatin. As shown in Figure 3a, gelatin-rich droplets without DNA coalesced with each other over time at 33 $^{\circ}\text{C}$. In con-

trast, the droplets entrapping DNA suppressed the coalescence (Figure 3b). We found that the presence of DNA stabilizes the droplets at elevated temperatures, even though the droplets were in the sol state.

3. Numerical Modeling

Numerical modeling was performed to assess the generation mechanism of different spatial patterns through the w/w phase separation in the capillary depending on the inner glass surface chemical affinity, as shown in Figure 1. In our previous study, we performed a simulation to interpret the different effects between tubule and planar-gap confinements on the w/w phase separation for an aqueous solution mixed with PEG and DEX by adapting the Cahn–Hilliard equation. Using the Cahn–Hilliard model, the formation of linearly-arranged DEX-rich droplets of almost the same size was well reproduced. However, for the planar-gap boundary, the size and morphology of the phase separation are rather random or dispersed in the experimental observation and numerical result. Thus, in this study, we extend the framework of the numerical modeling of our previous study based on the Cahn–Hilliard equation, Equation 1.

$$\frac{\partial \eta}{\partial t} = \nabla \cdot \left(M_c \nabla \frac{\delta F}{\delta \eta} \right) \quad (1)$$

where F is the free energy, t is time, and $M_c = (D_0/RT)$ is the diffusivity (D_0 is diffusion constant, R is universal gas constant and T is absolute temperature). The relative ratio of gelatin to the total PEG and gelatin is taken as the parameter η , where $\eta = [0, 1]$ and $\eta = 1$ corresponds to the state of 100% gelatin. The free energy F is given by

$$F = \int \left(RT[\eta \ln \eta + (1 - \eta) \ln (1 - \eta)] + L\eta (1 - \eta) + \frac{\alpha}{2} |\nabla \eta|^2 \right) dV \quad (2)$$

Where L , α , and dV are the interaction parameter, gradient energy coefficient, and differential volume, respectively. The first term in the parentheses corresponds to entropic contributions of mixing. The second term is the interaction energy, for which a parabolic relationship was adopted for simplicity and generality. The third term is instability due to the spatial gradient of η .

To incorporate the effect of boundary on the time development of the phase separation, we adapted the time-dependent Dirichlet condition^[38,39] by considering mass conservation. For simplicity, we adapted a 2D approximation to consider the effect of the inner surface of the glass capillary. The discrete domain and discrete boundary are defined as $\Omega^{\text{h}} = \{(x_i, z_j) | 1 \leq i \leq N_x, 1 \leq j \leq N_z\}$. Accordingly, the order parameter is spatially discretized as $\eta_{i,j}$. In the modeling of glass capillary experiments under a 2D approximation, we regard the x and z directions as the long-axis and cross-section of the glass capillary, respectively. In addition, we took the periodic boundary condition along the x -direction. As for the z -direction, we included the effect of different affinities of the glass surface for the time-stepwise calculations. For the boundary around the glass surface ($j = 1, 2$, and $N_z, N_z - 1$), we included the effect of the surface chemical-affinity between the gelatin and PEG. For example, for the solution adjacent to the surface of $j = 1$, we assumed the time-dependent

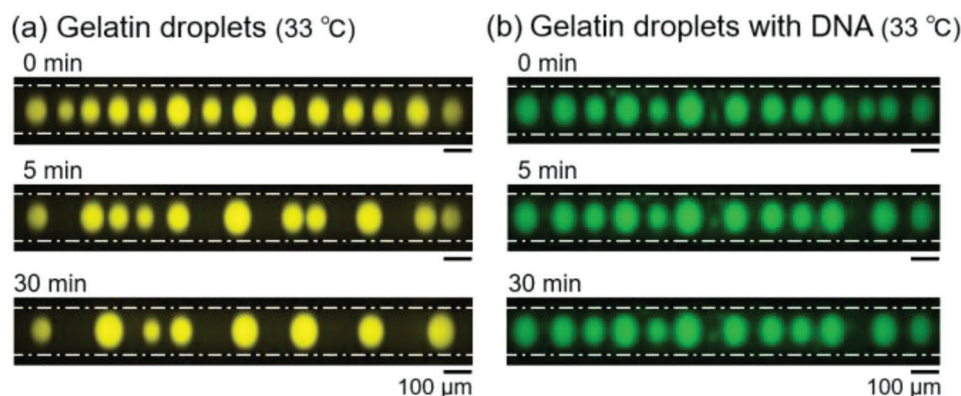


Figure 3. Effect of coexisting DNA on the size growth of gelatin-rich droplets following phase separation of PEG/gelatin solutions. Time evolution of gelatin-rich droplets at 33 °C (above the gelation temperature) within a capillary (inner diameter: 140 μm) introducing PEG/gelatin solution a) without or b) with DNA. Gelatin-rich droplets without DNA coalesced with each other and grew in size. In contrast, the gelatin-rich droplets entrapping DNA maintained their size over time.

change toward the preferable value of the parameter $\eta_{i,1}^0$ as a fixed value, with the simple kinetics as $d\eta_{i,1}^t/dt = k(\eta_{i,1}^0 - \eta_{i,1}^t)$ (k is kinetic constant). To fulfil the mass-conservation, the change of the layer with $j = 1$ was compensated by the change of that with $j = 2$.

$$\eta_{i,1}^{t+\Delta t} = \eta_{i,1}^t + k\Delta t (\eta_{i,1}^0 - \eta_{i,1}^t) \quad (3)$$

$$\eta_{i,2}^{t+\Delta t} = \eta_{i,2}^t - k\Delta t (\eta_{i,1}^0 - \eta_{i,1}^t) \quad (4)$$

$\Delta t = T_{\text{ime}}/N_t$ is the time step, T_{ime} is the final time, and N_t is the total number of time steps. The same time dependence was adapted for the other side of the boundary; η_{i,N_z}^t and η_{i,N_z-1}^t . In the actual simulation procedure, we have adapted the numerical step for Equations 1–4 in an alternative manner. Further detail of the numerical simulation is given in the Supporting Information.

Figure 4 shows the numerical results corresponding to time periods of circa 30 min. The order parameters are represented in the color gradient. The dark and light blue areas correspond to the gelatin-rich and the PEG-rich phases, respectively. Figure 4a shows the result with Equations 3 and 4 ($\eta_{i,1}^0 = \eta_{i,N_z}^0 = 0.15$) as the boundary condition corresponding to the PEG-coated capillary. The almost uniform cell-sized droplets were linearly arranged, whereas the results of the non-coating capillary with Equations 3 and 4 ($\eta_{i,1}^0 = \eta_{i,N_z}^0 = 0.55$), shown in Figure 4b, reproduces the adhesion of gelatin-rich droplets to the glass. The calculation with the boundary condition Equations 3 and 4 reproduces the experimental results as shown in Figure 1b,c. Note that the microphase separation remarkably depends on the surface chemical affinity of the inner glass surface.

4. Conclusion

Both experimental (Figure 1) and theoretical (Figure 4) results demonstrate that the wettability of the inner surface of the glass capillary dominated the pattern of w/w phase separation. By modifying the surface of a capillary with a higher affinity to PEG,

uniform cell-sized microgels are linearly and stably arranged in a self-organized manner through phase separation prior to the gelation of gelatin. As a result, the microgels can be extracted from the capillary into distilled water, maintaining their size. Furthermore, the size of microgels can be easily controlled by the inner diameter of the capillary. The mechanism of the microgels formation inside the glass capillary is explained as follows: initially, PEG- and gelatin-rich domains are formed by spinodal decomposition. Under the condition previously described, the PEG-rich phase is preferentially localized to the glass surface of the capillary because it has a higher affinity to the glass surface than the gelatin-rich domains. Consequently, gelatin-rich droplets are surrounded by the PEG-rich phase at the capillary center, and then gelation of gelatin inhibits the size growth of the polymer.

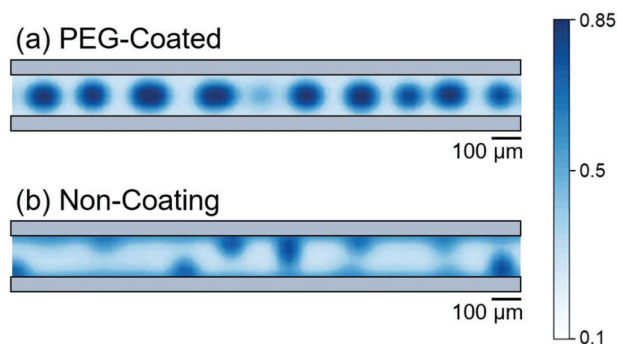


Figure 4. Theoretical modeling on the phase separation inside a capillary by taking into the effect of surface coating. The phase separation was calculated using the model equations (Equations 1 and 2) corresponding to periods of circa 30 min. For the boundary conditions on the surface of the capillary, Equations 3 and 4 were adopted. The dark blue in the color gradient corresponds to the gelatin-rich phase and the lighter areas to the PEG-rich phase. The gray area represents the glass wall of the capillary. a) For the surface that favors the PEG-rich solution ($\eta_{i,1}^0 = \eta_{i,N_z}^0 = 0.15$), uniform cell-sized droplets were linearly arranged. In contrast, b) the boundary condition along the surface was taken to prefer the gelatin-rich solution ($\eta_{i,1}^0 = \eta_{i,N_z}^0 = 0.55$), gelatin adhered to the glass, and the growth of droplets was prevented.

Microgels have a wide variety of properties and applications depending on their size and concentration, and the modification of the gelatin would also contribute to the structural stabilization of the microgels.^[40] It may be of scientific value to extend the current study to establish the optimal experimental conditions, such as composition, concentration, and modification of polymers to obtain the desired microgels.

The results shown in Figure 3 demonstrate that DNA molecules are spontaneously entrapped in the gelatin droplets, and the DNA contributes to maintaining the size of the droplets even above the sol/gel transition temperature. The negatively charged DNAs, that are incorporated in the droplets, may cause a negative electronic charge at the interface of droplets, which induces the stabilization of droplets by depressing the probability of fusion among droplets.^[19,20] This discovery may be valuable for using the cell-sized microgels as a cell model.

This study describes a method for producing uniform microgels by controlling phase separation and gelation of PEG/gelatin solutions confined in a glass capillary. Although the microfluidic method is applied to produce uniform microgels, it needs special equipment, such as tubing and pumps. For temperature control, a special set-up is required so as to maintain the entire apparatus to be a constant temperature. Furthermore, the solutions in the microfluidics are exposed to strong shear stress and mechanical stimuli that may break a long-stranded DNA. In fact, the breaking of a long-stranded DNA by mechanical agitation is reported.^[41] The current method does neither involve such a mechanical agitation nor cause the breakdown of a long-stranded DNA. It is highly expected that the present method will be applicable to the reconstruction and confinement in cell-sized droplets of genome-sized DNA, as well as toward the stable storage and transportation of these droplets. Therefore, the method proposed in our study, which does not require special equipment, organic solvents, or surfactants, may be useful for producing microgels for food, cosmetics, and other materials.

5. Experimental Section

The PEG with an average molecular weight (MW) of 20 000 was purchased from Fuji film Wako Pure Chemical Industries (Osaka, Japan). Alkali-treated (type-B) gelatin with an average MW of 6900 was obtained from Merck (Darmstadt, Germany). The MW of the alkali-treated (type-B) gelatin was determined by gel permeation chromatography. For fluorescence microscopy, gelatin was labeled with fluorescein isothiocyanate isomer I (FITC) (Excitation wavelength (Ex): 488 nm, Emission wavelength (Em): 530 nm, Sigma–Aldrich, St. Louis, MO, USA).

A glass capillary (Microcaps, Drummond, USA) with an inner diameter of 140 μm or 90 μm and 32 mm in the long axis was used to prepare the microgels. For PEG-coating of the inner wall of the glass capillary, Poly-L-Lysine graft PEG (PLL(20)-g[3,5]-PEG(2), SuSoS AG, Switzerland) was employed. PLL-g-PEG was dissolved in distilled water at 1 mg mL⁻¹ concentration and stored in aliquots at -20 °C until use. The glass capillary was treated with air plasma (PDC-32G, Harrick Plasma) at ≈ 400 mTorr for 5 min to improve the wettability to water before being filled with 100 $\mu\text{g mL}^{-1}$ of PLL-g-PEG solution. After incubating for 30 min at room temperature (≈ 24 °C), the glass capillary was washed with water and dried. The PEG-coated capillary was used within three days after being made.

PEG was dissolved in distilled water at 65 °C to make 3.4 wt vol⁻¹%, and then gelatin was added to make 4.5 wt vol⁻¹%. The solution was mixed using a vortex mixer until it became homogeneous and cloudy. The solution and glass capillary were incubated at 65 °C, which was higher than

the phase separation temperature.^[21,22] Immediately after the mixing, the solution was sucked up into a glass capillary, as shown in Figure 1a. Then, both ends of the capillary were sealed to avoid leakage and evaporation. The capillary containing the solution was quenched at room temperature (24 °C) to initiate the phase separation followed by the gelation of the gelatin-rich phase. The capillary was refrigerated at 5 ± 2 °C for four days to complete the gelation of gelatin-rich phase. The sealant on both ends of the cooled capillary was snapped off to extract the microgels from the glass capillary. The inner solution was pushed into 2 μL distilled water placed on a glass slide at room temperature (24 °C), as shown in Figure 2a.

DNA molecules from salmon sperm (500–1000 bp) were purchased from Fuji film Wako Pure Chemical Industries (Osaka, Japan). Gelred (Ex: 280 nm, Em: 600 nm, Biotium Inc., Fremont, CA, USA) was used as a fluorescent dye for the DNA. To investigate the localization and stabilization of DNA, DNA crystalline powder was dissolved in nuclease-free water. The solution was added to the PEG/gelatin solution in a homogeneous phase at 65 °C to be 80 μM and mixed using a vortex mixer. The capillaries were observed under a fluorescence microscope (Olympus BX51, Olympus Co.) on a horizontal stage and a heated stage (TPI-CKTS, Tokai hit, Shizuoka, Japan) to control the temperature of the capillary. The images were obtained with a Charge Coupled Device (CCD) digital camera (C11440-36U, Hamamatsu Photonics, Hamamatsu, Japan).

Both phase separation temperature T_p and gelation temperature T_g values for the composition (PEG/gelatin = 3.4 wt vol⁻¹%: 4.5 wt vol⁻¹%) were investigated by using microscopic observation and tilt tests. T_g and T_p were found to be 27 and 38 °C, respectively. These transition points were almost consistent with the previous reports.^[21] Also, neither the phase separation temperature nor the gelation temperature changed in the presence of 80 μM DNA.

Statistical Analysis: The results of Figure 2c were shown as box plots. As a pre-processing step, the experimental data were binarized using image-processing software (ImageJ, National Institutes of Health, USA), and the diameter was calculated from the area of circle. The mean \pm standard deviation (SD) and the number of microgels (n) used in the statistical analysis of the mean of microgel diameters were 61.7 ± 5.3 μm ($n = 5$) and 123.4 ± 19.2 μm ($n = 9$) for the ID 90 μm capillary and 140 μm capillary, respectively. The difference between the mean of microgel diameters extracted from the different capillary sizes was assessed by a paired t -test with two-sided tests and indicated by *** $p < 0.001$ (p is probability value). Microsoft Excel was used for statistical analysis.

Supporting Information

Supporting Information is available from the Wiley Online Library or from the author.

Acknowledgements

This work was supported by the Japan Science and Technology Agency (JST) toward creating the science and technology innovation fellowships (no. JPMJFS2145, M.S.) and the JST SPRING (no. JPMJSP2129, M.S.). The Japan Society funded this research for the Promotion of Science (JSPS) KAKENHI (no. 23KJ2081, M.S.), (no. JP20H01877, K.Y.), (no. 22H01188, M.Y.), and (no. 22K03560, A.S.), and the JST FOREST (no. JPMJFR213Y, M.Y.).

Author Contributions

M.S., M.Y., K.Y., and A.S. conceived this study. M.S. performed the experiments and analyzed the results. G.H., M.Y., and K.Y. designed the treatment for PEG-coating of glass capillaries. M.S. and K.Y. devised and performed numerical calculations. M.S. and A.S. wrote and summarized the manuscript with feedback from coauthors. All authors reviewed the manuscript.

Conflict of Interest

The authors declare no conflict of interest.

Data Availability Statement

The data that support the findings of this study are available from the corresponding author upon reasonable request.

Keywords

aqueous two-phase systems, uniform cell-sized microgels, water/water phase separation

Received: March 14, 2023

Revised: May 7, 2023

Published online:

- [1] S. Herianto, P.-J. Chien, J.-A. A. Ho, H.-L. Tu, *Biomater. Adv.* **2022**, *142*, 213156.
- [2] S. Hirschi, T. R. Ward, W. P. Meier, D. J. Müller, D. Fotiadis, *Chem. Rev.* **2022**, *122*, 16294.
- [3] T. Hamada, K. Yoshikawa, *Materials* **2012**, *5*, 2292.
- [4] P. Stano, *Life* **2018**, *9*, 3.
- [5] P. Schwille, J. Spatz, K. Landfester, E. Bodenschatz, S. Herminghaus, V. Sourjik, T. J. Erb, P. Bastiaens, R. Lipowsky, A. Hyman, P. Dabrock, J. C. Baret, T. Vidakovic-Koch, P. Bieling, R. Dimova, H. Mutschler, T. Robinson, T. D. Tang, S. Wegner, K. Sundmacher, *Angew. Chem., Int. Ed.* **2018**, *57*, 13382.
- [6] H. Udono, J. Gong, Y. Sato, M. Takinoue, *Adv. Biol.* **2022**, *7*, 2200180.
- [7] A. Kato, M. Yanagisawa, Y. T. Sato, K. Fujiwara, K. Yoshikawa, *Sci. Rep.* **2012**, *2*, 283.
- [8] M. B. C. De Matos, B. S. Miranda, Y. Rizky Nuari, G. Storm, G. Leneweit, R. M. Schifferers, R. J. Kok, *J. Drug Targeting* **2019**, *27*, 681.
- [9] Y. Shimane, Y. Kuruma, *Front. Bioeng. Biotechnol.* **2022**, *10*, 873854.
- [10] K. Takiguchi, M. Negishi, Y. Tanaka-Takiguchi, M. Homma, K. Yoshikawa, *Langmuir* **2011**, *27*, 11528.
- [11] M. Iqbal, Y. Tao, S. Xie, Y. Zhu, D. Chen, X. Wang, L. Huang, D. Peng, A. Sattar, M. A. Shabbir, H. I. Hussain, S. Ahmed, Z. Yuan, *Biol. Proced. Online* **2016**, *18*, 18.
- [12] J. R. SooHoo, G. M. Walker, *Biomed. Microdevices* **2009**, *11*, 323.
- [13] M. Tsukamoto, S. Taira, S. Yamamura, Y. Morita, N. Nagatani, Y. Takamura, E. Tamiya, *Analyst* **2009**, *134*, 1994.
- [14] Y. Chao, H. C. Shum, *Chem. Soc. Rev.* **2020**, *49*, 114.
- [15] Q. Ma, Y. Song, W. Sun, J. Cao, H. Yuan, X. Wang, Y. Sun, H. C. Shum, *Adv. Sci.* **2020**, *7*, 1903359.
- [16] A. T. Rowland, C. D. Keating, *Soft Matter* **2021**, *17*, 3688.
- [17] R. Mizuuchi, N. Ichihashi, *Chem. Commun.* **2020**, *56*, 13453.
- [18] H. Sakuta, F. Fujita, T. Hamada, M. Hayashi, K. Takiguchi, K. Tsumoto, K. Yoshikawa, *ChemBioChem* **2020**, *21*, 3323.
- [19] N. Nakatani, H. Sakuta, M. Hayashi, S. Tanaka, K. Takiguchi, K. Tsumoto, K. Yoshikawa, *ChemBioChem* **2018**, *19*, 1370.
- [20] K. Tsumoto, H. Sakuta, K. Takiguchi, K. Yoshikawa, *Biophys. Rev.* **2020**, *12*, 425.
- [21] M. Yanagisawa, Y. Yamashita, S.-A. Mukai, M. Annaka, M. Tokita, *J. Mol. Liq.* **2014**, *200*, 2.
- [22] M. Yanagisawa, S. Nigorikawa, T. Sakaue, K. Fujiwara, M. Tokita, *Proc. Natl. Acad. Sci. USA* **2014**, *111*, 15894.
- [23] S. Asakura, F. Oosawa, *J. Polym. Sci.* **1958**, *33*, 183.
- [24] M. Negishi, M. Ichikawa, M. Nakajima, M. Kojima, T. Fukuda, K. Yoshikawa, *Phys. Rev. E* **2011**, *83*, 061921.
- [25] E. Y. Basova, F. Foret, *Analyst* **2015**, *140*, 22.
- [26] S. Lee, J. de Rutte, R. Dimatteo, D. Koo, D. Di Carlo, *ACS Nano* **2022**, *16*, 38.
- [27] G. Zhang, J. Sun, *Int. J. Nanomed.* **2021**, *16*, 7391.
- [28] S. Sart, G. Ronteix, S. Jain, G. Amselem, C. N. Baroud, *Chem. Rev.* **2022**, *122*, 7061.
- [29] P. Zhu, L. Wang, *Chem. Rev.* **2022**, *122*, 7010.
- [30] K. O. Rojek, M. Ćwiklińska, J. Kuczak, J. Guzowski, *Chem. Rev.* **2022**, *122*, 16839.
- [31] M. Shono, R. Ito, F. Fujita, H. Sakuta, K. Yoshikawa, *Sci. Rep.* **2021**, *11*, 23570.
- [32] E. A. G. Jamie, R. P. A. Dullens, D. G. A. L. Aarts, *J. Chem. Phys.* **2012**, *137*, 204902.
- [33] M. C. Morán, N. Rosell, G. Ruano, M. A. Busquets, M. P. Vinardell, *Colloids Surf., B* **2015**, *134*, 156.
- [34] V. L. Truong-Le, S. M. Walsh, E. Schweibert, H. Q. Mao, W. B. Guggino, J. T. August, K. W. Leong, *Arch. Biochem. Biophys.* **1999**, *361*, 47.
- [35] M. Karg, A. Pich, T. Hellweg, T. Hoare, L. Lyon, J. Crassous, D. Suzuki, R. Gumerov, S. Schneider, I. Potemkin, W. Richtering, *Langmuir* **2019**, *35*, 6231.
- [36] F. Scheffold, *Nat. Commun.* **2020**, *11*, 4315.
- [37] Q. Feng, D. Li, Q. Li, X. Cao, H. Dong, *Bioact. Mater.* **2022**, *9*, 105.
- [38] Y. Li, D. Jeong, J. Shin, J. Kim, *Comput. Math. Appl.* **2013**, *65*, 102.
- [39] P. Benner, J. Heiland, *Science Open Research* **2015**, *1*.
- [40] Z. Gan, H. Liu, Y. Wang, T. Tao, M. Zhao, J. Qin, *Adv. Mater. Technol.* **2023**, *8*, 2201102.
- [41] H. Kikuchi, K. Nose, Y. Yoshikawa, K. Yoshikawa, *Chem. Phys. Lett.* **2018**, *701*, 81.